

Geotechnical assessment of a slope stability problem in the Citlakkale residential area (Giresun, NE Turkey)

Ayberk Kaya¹

Received: 14 December 2015 / Accepted: 4 May 2016 / Published online: 12 May 2016
© Springer-Verlag Berlin Heidelberg 2016

Abstract Because of the rapidly growing population, new settlement areas are required, and finding an appropriate location is always difficult, especially in mountainous areas. In these regions, efficient use of the existing settlement areas or rehabilitating unsuitable areas for settlement is the most common application. The Citlakkale (Giresun-NE Turkey) District residential area, located on a steep slope where debris crops out, was selected as an application site for this study. Following the slope excavation to establish a new settlement in the study area, an instability problem occurred. In order to investigate the causes and mechanism of the failure and to determine the remedial measures, detailed geotechnical studies were performed. Inclinator measurements revealed that it is a composite sliding with a very slow velocity. Stability of the slope debris was investigated using limit equilibrium (LE) and the finite element method-based shear strength reduction (FEM-SSR) analyses in three stages. These were slope stability analyses for pre- and post-excavation cases and possible remedial measures. According to the stability analyses, the slope excavation was found to be major factor in the occurrence of the failure. Based on the gathered data, retaining wall having a lateral active force higher than 9524 kN was considered to be economical and practical solution as a remediation method. Furthermore, integrating the LE and FEM-SSR methods give useful and reasonably reliable results in assessing the stability of soil slopes.

Keywords Slope stability · Excavation · LE and FEM-SSR methods · Remediation

Introduction

Mass movement is one of the most damaging and costly natural hazards of the earth that occur abruptly and cause significant damage. Every year worldwide, this process causes deathly casualties and remarkable direct and indirect economic losses. Over the past 30 years, international research institutions and many governments in the world have expended notable amount of resources in appraising mass movement hazards (Guzzetti et al. 1999).

In Turkey, particularly in the eastern Black Sea region (EBSR) (Fig. 1), many mass movements occur frequently and cause monetary losses annually. In the literature it was reported that the high frequency of heavy rainfalls, steep slopes, weathering, and human activities are the main triggering factors for mass movements observed in EBSR (e.g. Genc 1993; Bulut et al. 2000; Akgun and Bulut 2007; Yalcin and Bulut 2007; Akgun et al. 2008; Kesimal et al. 2008; Yalcin 2008; Karsli et al. 2009; Akgun 2011; Nefeslioglu et al. 2011; Nefeslioglu and Gokceoglu 2011; Reis et al. 2012; Alemdag et al. 2013, 2014, 2015; Karaman 2013; Karaman et al. 2013; Avsar et al. 2014; Osna et al. 2014; Kaya et al. 2015, 2016; Topsakal and Topal 2015). Because of the growing population, new settlement areas are required in mountainous areas of EBSR. The preliminary geotechnical works are not generally performed for the selection of settlement areas. Therefore, each human activity impacts the environment doing changes in the stress conditions, natural balance, and natural morphology. As a result, many stability and engineering problems have occurred in this region and

✉ Ayberk Kaya
ayberk.kaya@erdogan.edu.tr

¹ Department of Geological Engineering, Faculty of Engineering, Recep Tayyip Erdogan University, 53100 Rize, Turkey

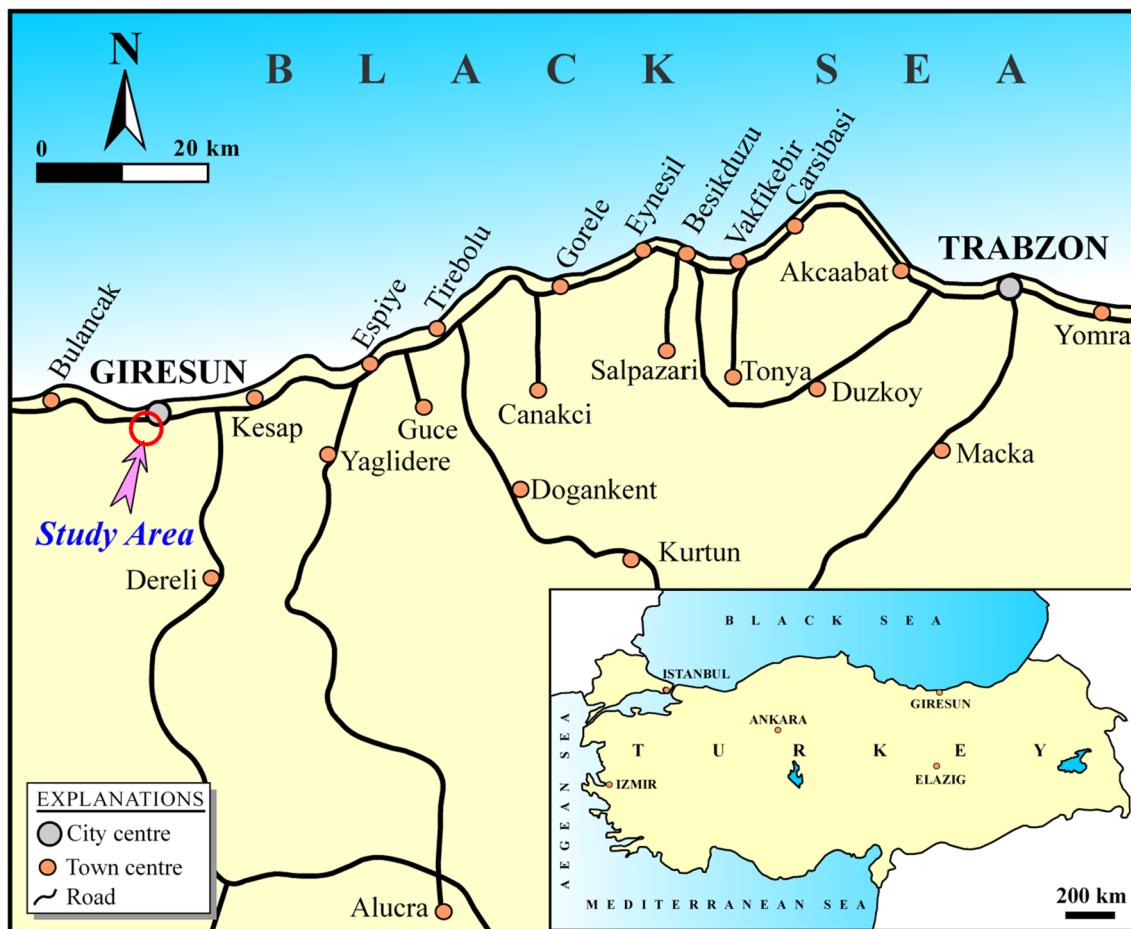


Fig. 1 Location map of the study area

threatened the residents. Following the slope excavation with an approximate length of 100 m and a height of 13 m (Fig. 2a) to obtain a new settlement area in Citlakale District located in mountainous area of EBSR where the incline of slope is approximately 20° , an impending failure occurred in late-March 2014. This failure damaged 12 houses, caused developing of cracks on the ground, tilting of fences and tree bodies (Fig. 2b–g). Therefore, detailed geotechnical studies including field measurements, laboratory studies, and slope stability analyses were carried out to understand the occurrence mechanism of the failure and to determine the triggering factors and reliable remedial measures needed to stabilize the region.

Geology of the study area

Eastern Pontide is subdivided into southern and northern zones (Ketin 1966) on the basis of lithological and structural evidence. The study area is situated in the northern part of the Eastern Pontide Tectonic Assembly, Black Sea

Region, Turkey. The geological map of the study and surrounding area is drawn and depicted in Fig. 3.

The Late Jurassic–Early Cretaceous aged Berdiga Formation conformably overlies the Late Cretaceous–Paleocene aged volcanic sedimentary rocks. These rocks comprise four units, namely the Catak, Kizilkaya, Caglayan, and Bakirkoy formations, separated by their rock associations. The Eocene aged Kabakoy Formation is widely outcropped in the northern zone of the Eastern Pontide. Quaternary alluvium and slope debris are the youngest units in the area (Guvenc 1993).

Geological units of the Kizilkaya Formation are widely cropped out along the N–S direction in the area. This formation is composed of rhyodacite, dacite, and their pyroclastites with clayey and sandy limestone intercalations. The rocks are generally well jointed, while fresh surfaces are white, beige, or whitish gray on weathered surfaces. Dacitic and rhyodacitic rocks are characteristically brownish, reddish, and yellowish or buff colored.

Kizilkaya Formation overlies the studied debris unit consisting of tabular, angular, and sometimes less round-

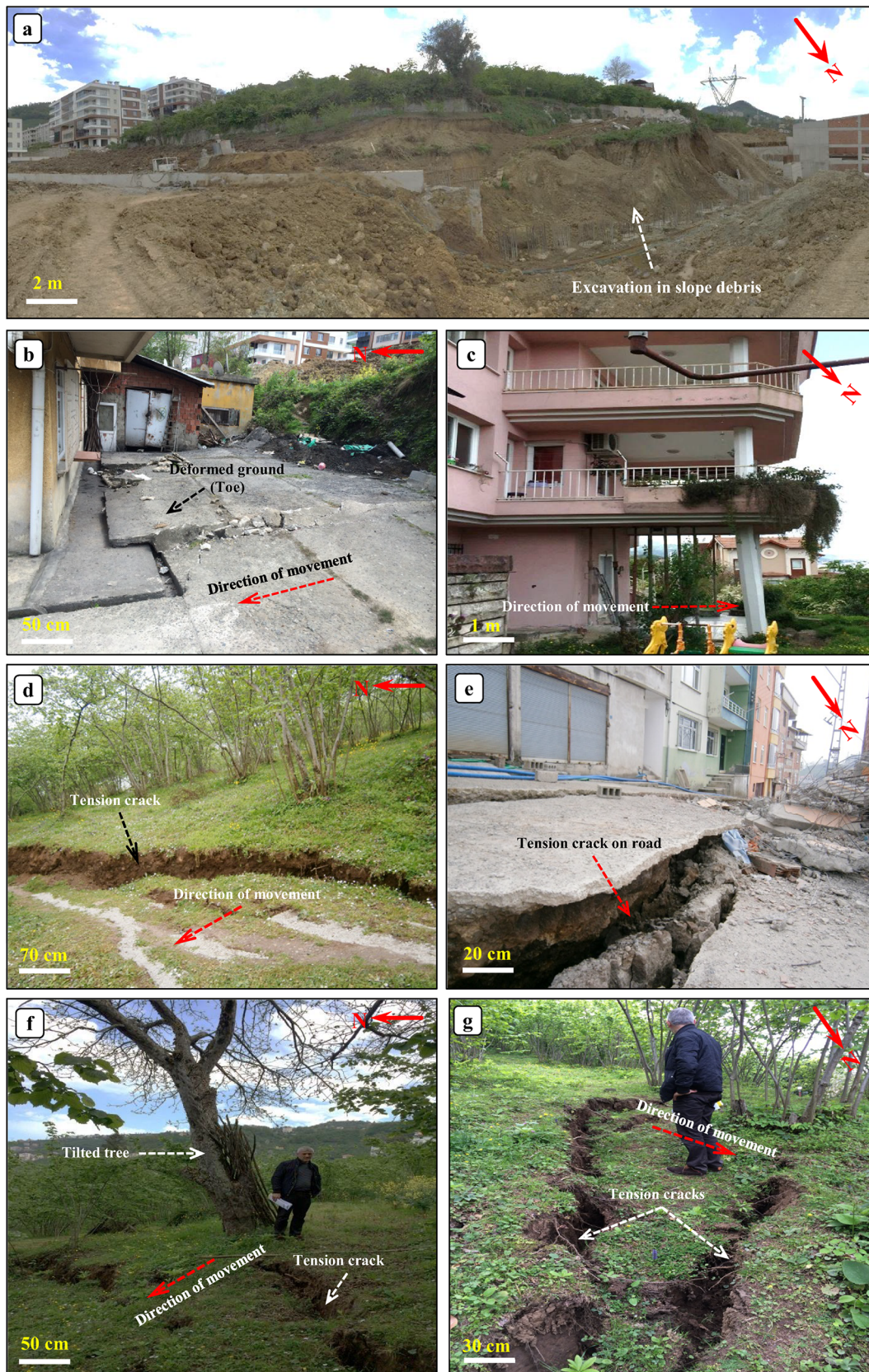


Fig. 2 a Slope excavation, b, c deformations on the houses and d–g tension cracks on the ground formed by mass movement in the study area

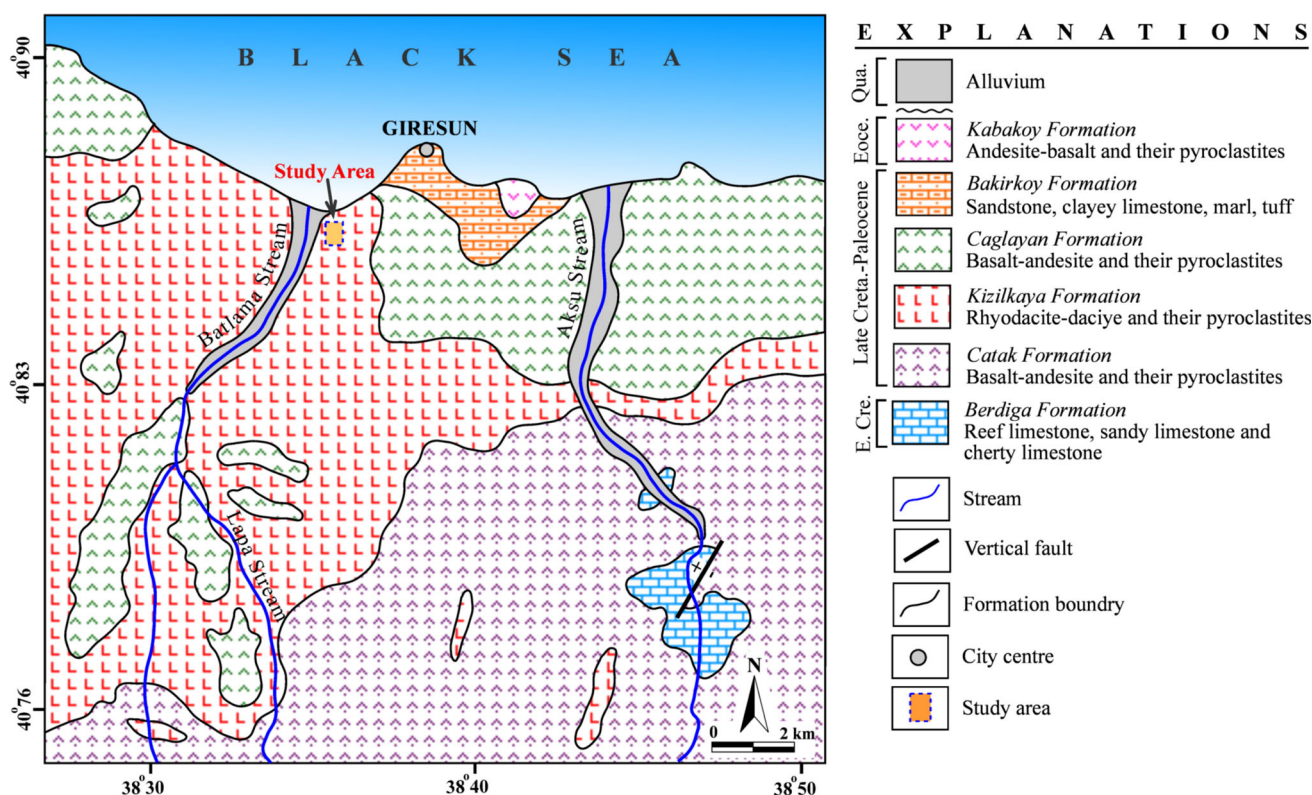


Fig. 3 Simplified geological map of the close vicinity of the study area (Modified from Guven 1993)

shaped gravels and blocks that are composed in general of limestone and basalt. Contents of the gravels and blocks in different lithology unlike the acidic rocks of Kizilkaya Formation prove that it has been transported away from its original place. The amount of clay, silt, and sand is more abundant than gravel and block materials.

Geotechnical studies

Data collection was performed by means of surface and underground studies. Geotechnical properties of the slope debris were determined based on the field observations/measurements, laboratory tests, and back analyses. In total, 12 boreholes were drilled within the study area. All boreholes were used for inclinometer measurements, ground water level and depth of bedrock determinations, and sampling. Laboratory tests such as particle size distribution, consistency limits, unit weight, and triaxial tests were carried out on these samples. In three profiles, seismic refraction studies were performed. The detailed information obtained from geotechnical studies are given below.

Borehole investigations

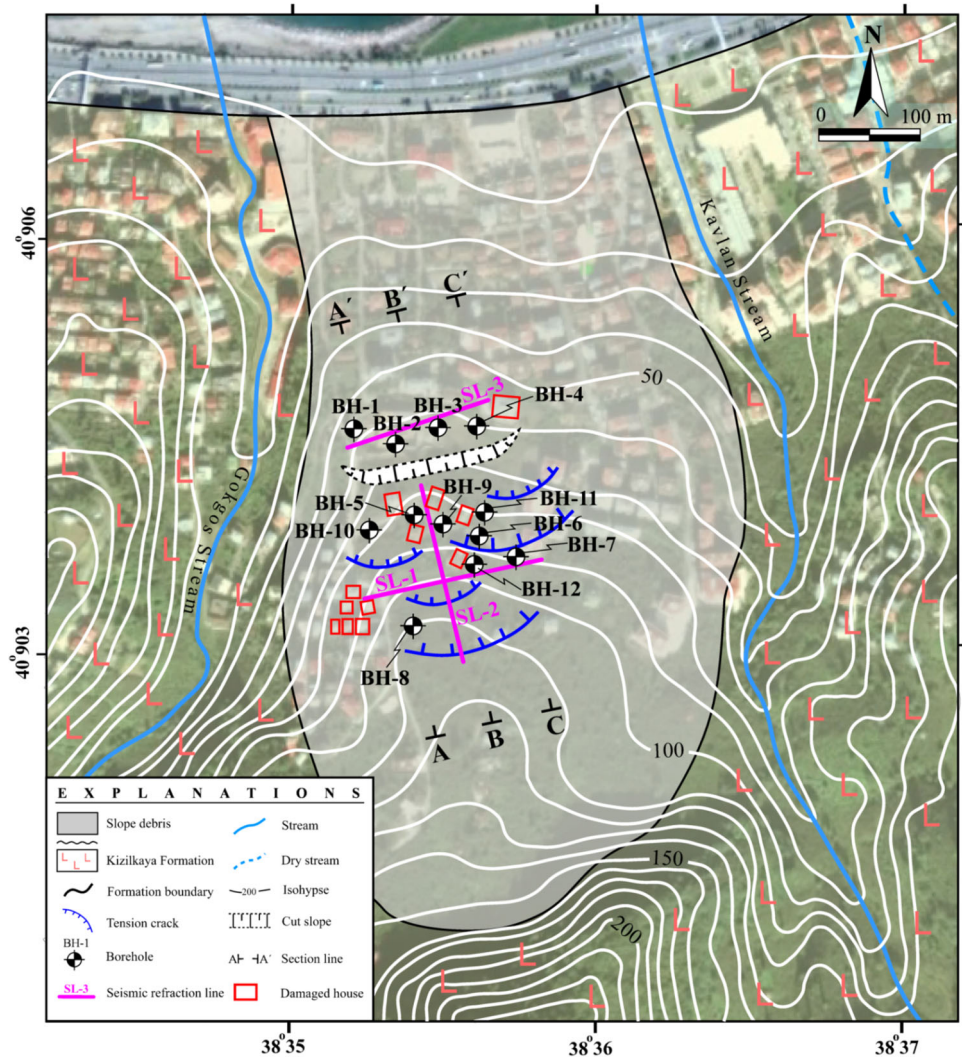
Twelve boreholes with a total length of 301 m were drilled in order to investigate the ground water level, variation in

the thickness of the slope debris, execute inclinometer measurements, and undisturbed/disturbed sampling (Figs. 4, 5). The data obtained from the investigation boreholes showed that the slope debris consisting of clay, silt, sand, and gravel-sized particles, has a thickness ranging from 10 to 18 m, and Kizilkaya Formation overlies the debris unit. The ground water exists at a depth between 8.3 and 17.0 m. The depth of boreholes, thickness of slope debris, and ground water level are presented in Table 1.

Geophysical investigations

The geophysical studies were carried out by using the seismic refraction method in three lines in order to determine the dynamic deformation modulus (E_{dyn}) and Poisson's ratio (ν_{dyn}) of the slope debris found in the Citlakale District residential area (Fig. 4). Seismic refraction is a geophysical exploration method which uses the basis of seismology to estimate the properties of the earth's subsurface using the refracted seismic waves. This method has been also successfully used to investigate the subsurface features such as discontinuity detections, stratigraphic relationships, karst problems, and depth of bedrocks. By performing the seismic studies using a 12-channel Geometrics ES3000 model seismograph, primary-wave (V_p) and secondary-wave (V_s) velocities were determined. As the results of seismic refraction studies were assessed, the

Fig. 4 Engineering geological map of the study area



V_p velocities for each Seismic Refraction Line (SL-1, SL-2, SL-3) were found to be 667, 885, 479, and 290, 354, 252 m/s for V_s , respectively. These data obtained from the seismic refraction method was used in calculation of the dynamic elastic parameters (E_{dyn} and v_{dyn}) of slope debris. The E_{dyn} and v_{dyn} values, which are necessary inputs in numerical slope stability analyses were calculated with the help of following equations proposed by Bowles (1988);

$$E_{dyn} = V_s^2 \left[\frac{3 V_p^2 - 4 V_s^2}{(V_p^2 - V_s^2)} \right] \tag{1}$$

$$v_{dyn} = (V_p^2 - 2 V_s^2) / 2 (V_p^2 - V_s^2) \tag{2}$$

where V_p ; primary-wave velocity (m/s) and V_s : secondary-wave velocity (m/s).

As a result, the average E_{dyn} and v_{dyn} values were calculated to be 25.03 GPa and 0.32, respectively.

Inclinometer measurements

The subsurface location of a landslide can be detected with an inclinometer. The monitoring instruments are installed within a borehole and can then take regular measurements to determine the variation of the mass movements so that the movement is recorded by data loggers.

To determine the subsurface location of the failure, all boreholes were outfitted with the inclinometers and measurements were recorded at every 50 cm interval. The direction of the mass movement was obtained using the movement vectors produced from the inclinometer measurements. Table 2 shows the displacement measurements that were taken from all boreholes. All measurements showed that the failure surface is located at depths between 3.4 and 12.0 m. An example of the cumulative displacement graph for BH-8 is presented in Fig. 6. The slide

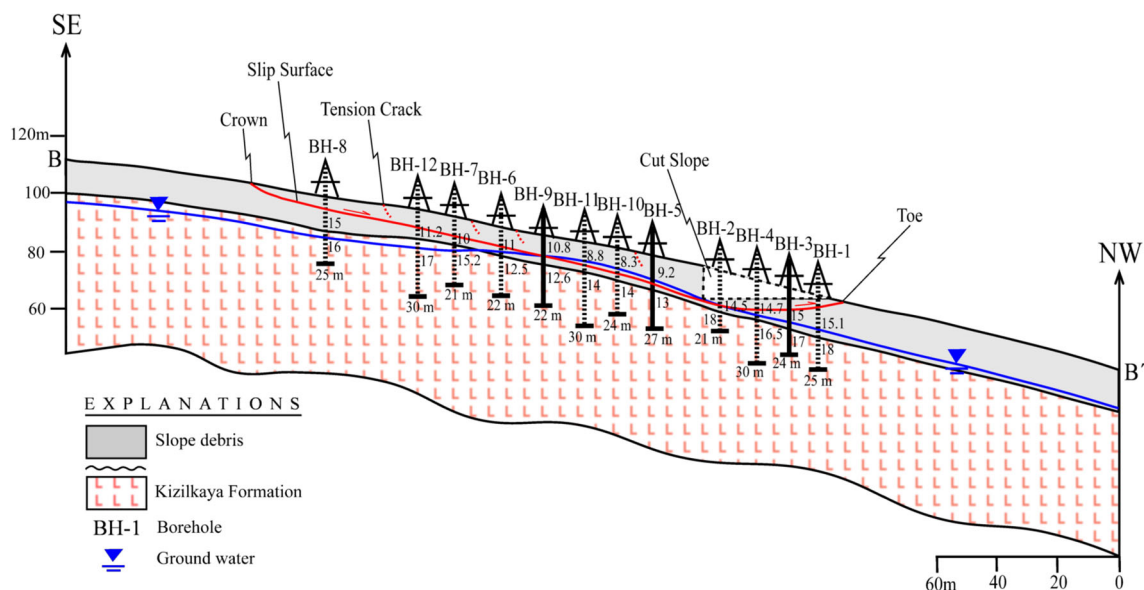


Fig. 5 B–B' cross-section showing the soil profile and slip surface

Table 1 Summary of the borehole data

Borehole no.	Borehole depth (m)	Borehole elevation (m)	Slope debris thickness (m)	Ground water depth (m)
BH-1	25.0	58	18.0	15.1
BH-2	21.0	65	18.0	14.5
BH-3	24.0	63	17.0	15.0
BH-4	30.0	60	16.5	14.7
BH-5	27.0	83	13.0	9.2
BH-6	22.0	87	12.5	11.0
BH-7	21.0	89	10.0	15.2
BH-8	25.0	110	15.0	16.0
BH-9	22.0	85	12.6	10.8
BH-10	24.0	73	14.0	8.3
BH-11	30.0	79	14.0	8.8
BH-12	30.0	95	11.2	17.0

movement is about 0.65 mm/day along the NW direction considering the average rate for the period of the field investigation. According to landslide movement classification proposed by Varnes (1978), the mass movement in Citlakkale District is described as “very slow” in terms of its average daily velocity value. The inclinometer measurements also provided important information about the failure mode of this failure. Correlation of the inclinometer measurements indicated that, this is a slide with composite (circular + linear) failure surface (Fig. 5).

Laboratory studies

Laboratory studies were carried out on disturbed and undisturbed soil samples taken with Shelby tubes to

determine the physico-mechanical properties of the debris unit. Natural and saturated unit weights, consistency limits, and shear strength parameters were measured on these samples. The index properties, particle size distribution, and consistency limits belong to debris unit were determined according to ASTM (2009a, 2009b, 2010) standards. Considering the particle size analyses of all samples, there was 0–19 % of gravel, 15–41 % sand, 34–53 % silt, and 12–39 % clay size particles in the soil specimens taken from the study area. Samples were categorized according to USCS (Unified Soil Classification System) (ASTM 2011a) and the slope debris in the study area was classified as MH (high plasticity silt), CH (high plasticity clay), and SM (silty sand).

Table 2 Summary of the inclinometer measurement results

Borehole no.	Borehole depth (m)	Inclinometer casing (m)	Slip surface (m)	Displacement amount (mm)	Measurement duration (days)	Rate (mm/day)
BH-1	25.0	23.5	2.5	46.4	58	0.8
BH-2	21.0	21.0	2.5	47.2	59	0.8
BH-3	24.0	23.0	3.0	18.6	62	0.3
BH-4	30.0	30.0	3.0	34.8	58	0.6
BH-5	27.0	11.0	10.5	55.8	62	0.9
BH-6	22.0	10.0	10.0	55.8	62	0.9
BH-7	21.0	20.5	8.0	30.5	61	0.5
BH-8	25.0	22.5	3.5	31.8	60	0.5
BH-9	22.0	17.5	10.0	42.2	60	0.7
BH-10	24.0	23.5	9.0	33.6	56	0.6
BH-11	30.0	29.0	9.5	44.8	56	0.8
BH-12	30.0	29.5	7.0	26.4	66	0.4

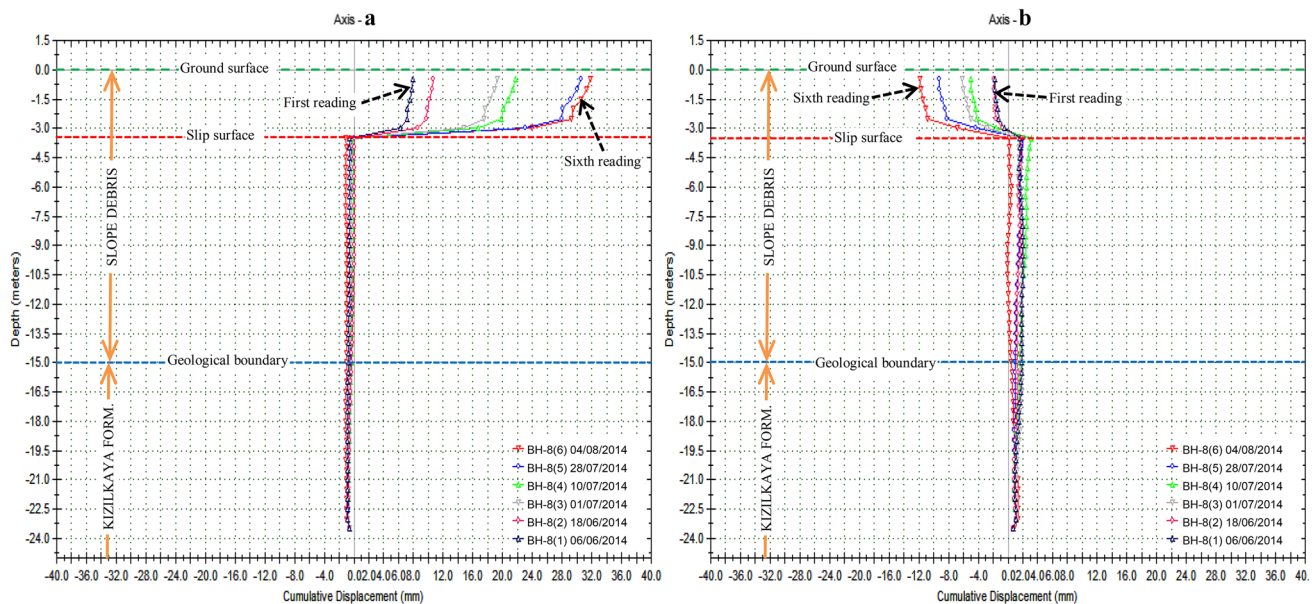


Fig. 6 Cumulative displacement of the BH-8

As it is known, after an excavation is made for cut, the shear stress of soil is induced that may bring about its failure in the undrained state. In this case, the peak shear strength parameters of unfailed slope can be defined by undrained tests. Therefore, in this study, the triaxial tests were performed under consolidated-undrained (CU) conditions on the undisturbed soil samples considering the ASTM (2011b) standard in order to determine the cohesion (c) and internal friction angle (ϕ). According to CU test, the c and ϕ values were found to vary between 36.3–60.1 kPa and 8°–15°, respectively. The results of the laboratory tests are summarized in Table 3.

Back analyses

The shear strength parameters of the failed landslide body were determined from the limit equilibrium back analysis method using the multiple solution of Sancio (1981). Back analyses were performed along the selected A–A', B–B', and C–C' sections shown in Fig. 4, which were parallel to the movement direction. In this method, assuming the limit equilibrium condition (FOS = 1), the effective residual c' and ϕ' values are satisfied. Taking into account the composite shape of the failure surface, the back analysis of the slope was carried out using the Janbu Method (Janbu 1973)

Table 3 The distribution of soil classifications and the geotechnical properties for the soil samples

Borehole no.	Sample no	γ_n (kN/m ³)	γ_s (kN/m ³)	% retained 4 no. sieve	% passed 200 no. sieve	LL (%)	PL (%)	PI (%)	USCS	C (kPa)	ϕ (°)
BH-2	1	17.3	18.3	0	50.0	56	34	22	MH	49.1	12
BH-3	1	17.5	18.4	1	84.0	52	28	24	CH	58.9	8
	2	17.5	18.5	4	14.9	–	–	–	SM	–	–
BH-4	1	17.8	18.9	3	80.3	62	31	31	MH	57.9	9
	2	17.6	18.5	6	21.6	–	–	–	SM	–	–
BH-5	1	18.1	19.2	1	50.4	51	30	21	MH	47.1	13
	2	17.6	18.4	6	20.3	–	–	–	SM	–	–
BH-6	1	17.2	18.1	9	59.6	58	31	27	MH	59.8	9
	2	17.5	18.5	10	50.0	45	26	19	SC	42.2	15
BH-7	1	18.6	19.7	1	76.0	51	27	24	CH	60.1	8
BH-8	1	17.7	18.8	4	88.0	66	36	30	MH	55.9	9
	2	17.7	18.9	19	50.0	55	31	24	SM	36.3	15
Min.–Max.	–	17.3–18.6	18.1–19.7	0–19	88.0–14.9	45–66	26–36	19–31	–	36.3–60.1	8–15
Ave.	–	17.7	18.7	5	53.8	55	30	25	–	51.9	10.9

LL liquid limit, PL plastic limit, PI plasticity index, γ_n natural unit weight, γ_s saturated unit weight, c cohesion, ϕ internal friction angle

by means of Slide v6.0 (Rocscience Inc. 2010) software. The probabilistic analysis was applied to perform the back analysis of two variables at the same time. Furthermore, in order to get more reliable and realistic results, static loads owing to surrounding buildings were taken into account and tension cracks were added. The effective residual cohesion and internal friction angle values were found to be 6 kPa and 12.5°, correspondingly from the back analyses (Fig. 7).

Finally, the shear strength parameters obtained from back analyses were compared with the laboratory shear strength parameters. Comparison of the shear strength parameters reveals that a higher cohesion value was attained from the laboratory tests as expected. The main reason for this difference is due to the drainage of the ground water. In CU tests, no water drainage takes place during the shearing and pore pressure builds up. However, it is assumed that soil slopes fail under drained conditions in back analysis method. Therefore, the shear strength parameters obtained from CU tests were used in the short-term stability analyses of the unfailed slope body and back analyses results were used in the long-term stability analyses of the failed slope.

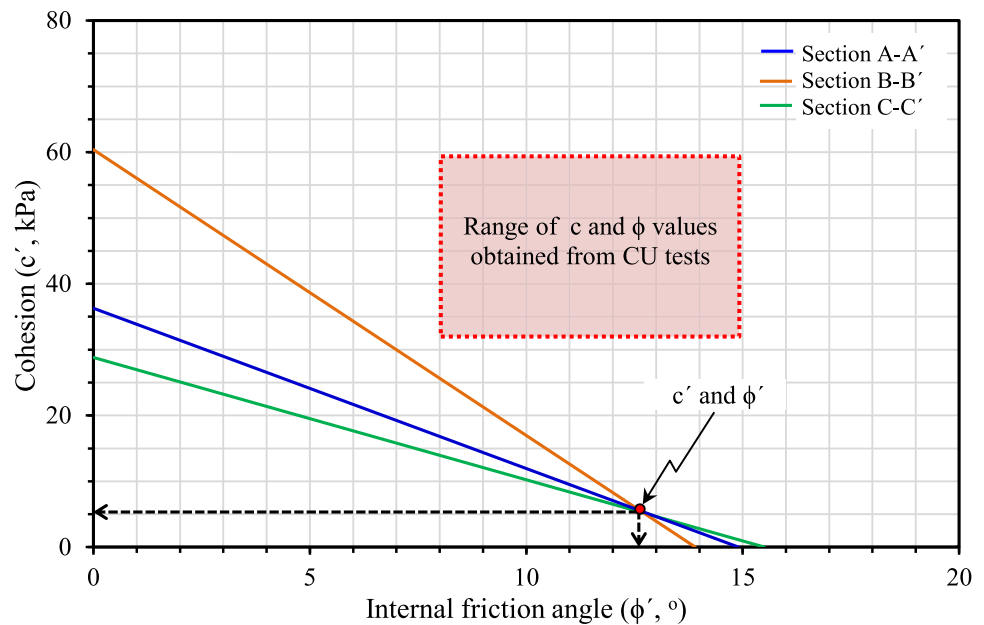
Assessment of slope stability

In the literature, stress analysis, limit equilibrium, empirical, numerical, and physical methods are commonly used to determine the stability of the soil slopes (e.g. Fellenius 1936; Janbu 1954a, b; Bishop 1955; Bishop and Morgenstern 1960; Lowe and Karafiath 1959; Morgenstern and

Price 1967; Spencer 1967; Janbu 1968, 1973; USCE 1970; Sarma 1973; Fell et al. 1996; Griffiths and Lane 1999; Shukra and Baker 2003; Hammah et al. 2006; Li 2007; Hart et al. 2008). These researchers have used different methods in their studies which were conducted at either local or regional scale according to the type of problem and the properties of the soil. As these studies assessed, it is seen that the limit equilibrium and finite element methods are the most preferred by researchers. In limit equilibrium (LE) method, which accounts for an important part of the slope stability analysis methods, Mohr–Coulomb failure criterion suggested by Mohr (1900) is predicated; a surface having a failure possibility is chosen and the stress condition that would cause the failure along this surface is investigated. Then the shear stress that keeps the mass in shear zone in equilibrium is calculated. The calculated stress values are compared and factor of safety (FOS) is determined accordingly (Alemdag et al. 2015). Numerical stability analysis methods are useful tool that allow designers to compare and control the validity of LE analyses results. Because of the rapid advances in computer systems, FEM-SSR (finite element method-shear strength reduction) technique based software is increasingly used today. In FEM-SSR method, the elastic parameters and forces acting on a slope forming material are also considered, unlike in the LE method.

In order to investigate the stability of the slope debris and necessary measurements within the study area, the LE and FEM-SSR analyses were evaluated together on the B–B' cross-section using the Slide v6.0 (Rocscience Inc. 2010) and Phase² v8.0 (Rocscience Inc. 2011) computer packages, respectively. Slide is a computer software that is

Fig. 7 c' – ϕ' graph of the slope debris showing the back analysis results



frequently used for the calculation of FOS value for soil slopes based on the LE method. The surfaces having different lithological characteristics and geometry can be modeled in both simple and complex form by this software. Slide also allows the users to define and analyze a ground water problem using the same model as for the slope stability problem. Phase² is a powerful and flexible software, which uses the shear strength reduction (SSR) method combined with the FEM and interpretation modules. In the FEM-SSR method, the factor of safety (FOS) is symbolized by the strength reduction factor (SRF). The SSR method involves methodical use of FEM to determine a SRF value that brings a slope to the verge of failure. The shear strength parameters are scaled until the stability limit is reached. The SRF value is the ratio between the actual and the model strength at the stability limit. One of the advantages of the SSR method is that there is no need to the primary guess at definition of critical failure surface (Kaya et al. 2015).

To understand the generation mechanism of the failure and, to determine the triggering factors and the remedial measures, the LE and FEM-SSR analyses were carried out in three stages as follows.

Slope stability analysis for the pre-excitation case

In the first step, pre-excitation geometry of the slope was modelled in the Slide software. The Mohr–Coulomb failure criterion was chosen in the analysis model. The Janbu Method (Janbu 1973) was preferred in LE analysis since the length of the slope debris is bigger than its thickness and it has a composite slide hazard. The static load due to

surrounding buildings was added into the model. For the case of unfailed slope body, the shear strength parameters of c 51.9 kN/m³ and ϕ 10.9° obtained from CU tests were used. The soil below the ground water table was assumed to be saturated, thus saturated unit weight value of 18.7 kN/m³ was inserted for this zone. According to the LE analysis, the FOS value of the slope having natural topographical geometry was determined as 1.272 (Fig. 8a).

In the second step, same model was analyzed in Phase² software in order to control the result of LE analysis. In the analysis model, finer zoning was applied and six-nodded triangular finite elements were chosen in the mesh and the Mohr–Coulomb failure criterion was applied. E_{dyn} and ν_{dyn} parameters obtained from the seismic refraction studies were used in the model. Since the elastic-perfectly plastic (EPP) model best replicates the LE analysis, slope debris was considered to be EPP material and continuum media. According to the FEM-SSR analysis performed, the SRF value was found to be 1.29 (Fig. 8b).

It is very clear that the FOS values obtained from LE and FEM-SSR analyses for pre-excitation case were nearly same and greater than limit equilibrium (FOS = 1) condition. Thus, any failures were not expected to occur for the natural topographical geometry and the slope was stable for pre-excitation case.

Slope stability analysis for the post-excitation case and determination of critical slope height

It is important to know the effects of high steep slope excavations on stability in terms of understanding the causes and mechanism of the failure. Therefore, firstly, the

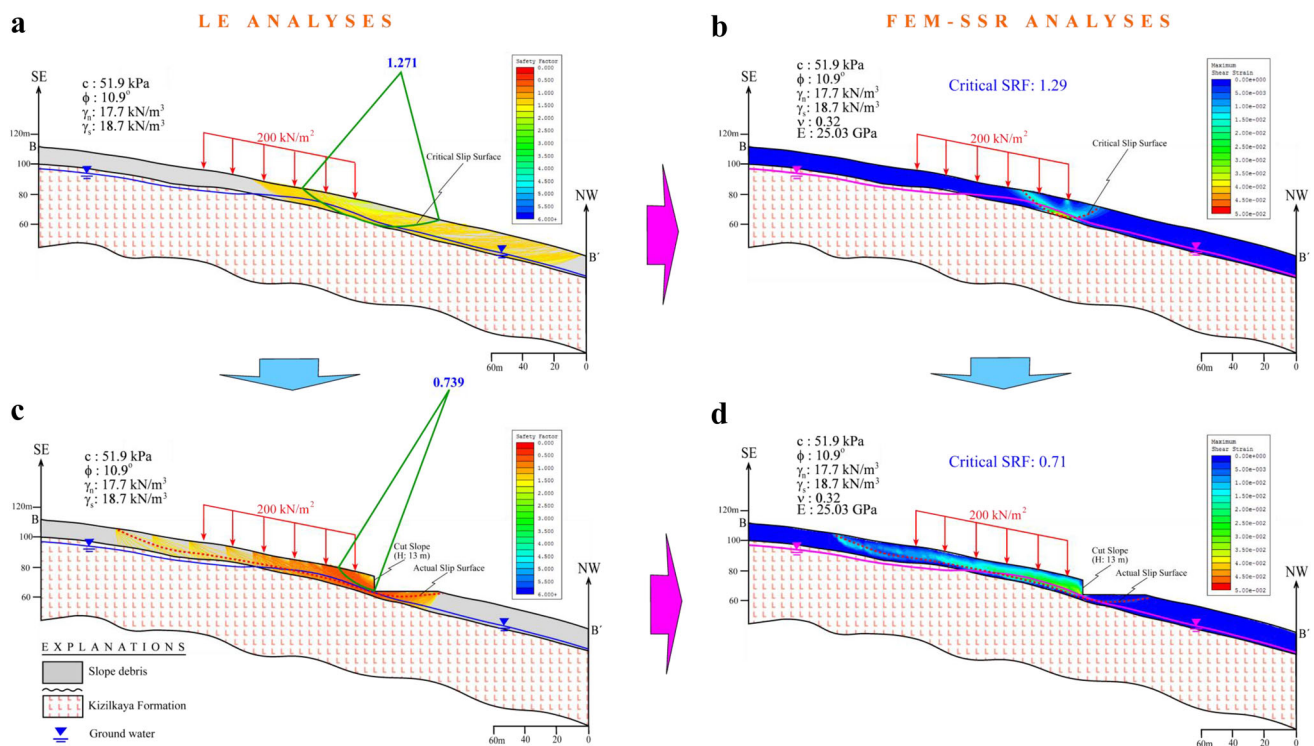


Fig. 8 LE (a, c) and FEM-SSR (b, d) analyses evaluated for pre- and post-excitation cases along the B–B' cross-section

analyzed models having different slope heights varying between 1 and 13 m with close to right angles were generated using the Slide software in order to determine the critical slope height ($H_{critical}$) of debris unit crops out in study area. In this stage, to define the short-term conditions for each unfailed slope model, the shear strength parameters obtained from CU tests were considered and the Mohr–Coulomb failure criterion was employed in the Janbu Method. Furthermore, the soil below the ground water table was considered to be saturated and the building-induced static loads were added same as the pre-excitation analysis model. Secondly, the same models were analyzed in Phase² computer package to control the accuracy of LE results. An example of the LE and FEM-SSR analyses for the cut slope with 13 m height is presented in Fig. 8c, d. As can be seen in Fig. 8c, the possible failure surfaces with a safety factor smaller than one ($FOS < 1$) obtained from LE analysis are located in the landslide affected area. Considering the FEM-SSR analysis, the maximum deformations develop around the actual failure surface obtained from inclinometer measurements (Fig. 8d). Results of the LE and FEM-SSR analyses completely coincide with the actual situation observed in the field.

According to LE analyses, the $H_{critical}$ value was found to be 8 m based on the limit equilibrium condition ($FOS = 1$) and FOS values over the critical height of 8 m were tended to decrease (Fig. 9). It was also concluded that

the FOS values were remained constant at a value of 1.272 for slope heights lower than 4 m. However, the $H_{critical}$ value was determined as 6.5 m according to FEM-SSR analyses (Fig. 9). Since forces acting on a slope forming material and elastic parameters are also taken into account in FEM-SSR method, the result of the FEM-SSR analysis seems to be more realistic than the LE analysis result. These results show that the slope will be unstable over the height of 6.5 m if it is not supported.

Therefore, some special measures were needed to prevent the effects of the failure and to stabilize the affected area.

Remedial measures

In the literature, there are various landslide remediation methods include bridging, buttressing, flattening, reinforcement, rerouting, retaining walls, soil hardening, surface and subsurface drainage, surface slope protection, thermal treatment, unloading, and vegetation. (Turner and Schuster 1996; Abramson et al. 2001; Ontigao and Sayao 2004; Duncan and Wright 2005; Fahimifar et al. 2013). Because there is insufficient area for flattening, the retaining wall was selected as the most economic and reliable reinforcement type for the failed slope. In retaining wall projects, determination of the lateral earth pressure distributions is very important in terms of safety and cost.

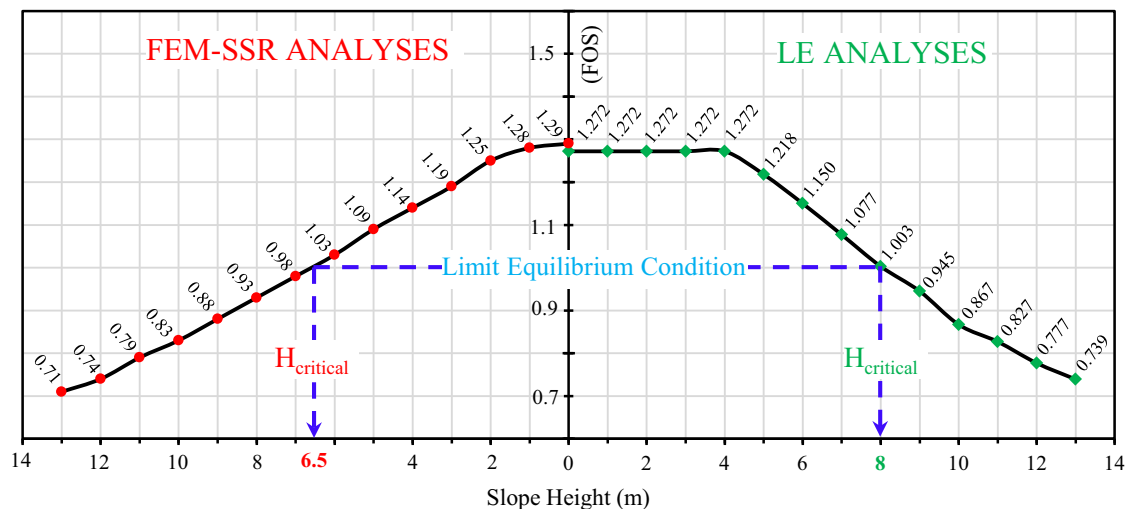


Fig. 9 The graph showing the $H_{critical}$ value based on the LE and FEM-SSR analyses evaluated for different slope heights

Therefore, the lateral active force needed to be applied to make the region stable should be identified before the construction phase.

In order to determine the lateral active force, the Slide software was used by means of LE method considering the analysis model having a slope height of 13 m showing the actual situation. The long-term stability model under a pseudo-static seismic load and fully saturated case was analyzed using the Janbu Method. Furthermore, the tension cracks, composite slip surface and static loads were added into the model. In long-term stability analyses, the soil slopes are analyzed using drained strengths expressed in terms of effective stress parameters. Back analysis of slope failures is an effective means of determining residual strengths of failed slope body. Therefore, the effective shear strength parameters attained from the back analyses were used in the analysis model.

The Black Sea Fault beneath the sea which is approximately 15 km away from Citlakkale District was taken into account in seismic load calculation (Fig. 10). According to earthquake catalogue prepared by Turkish Disaster and Emergency Management Authority, seven earthquakes that originated Black Sea Fault have occurred with a magnitude larger than five ($M_w > 5.0$) within last 50 years (AFAD 2016). The largest of them was 1968 Amasra-Bartın earthquake with a magnitude of $M_w = 6.6$ in which 29 people were killed. In determination of the design ground motion parameters, an earthquake with a magnitude of $M_w = 6.0$ was considered. Taking into account the distance of the Black Sea Fault and type of ground (soft soil), the peak ground acceleration (PGA) value was determined to be 0.18 g using the Ulusay et al. (2004) attenuation relationship suggested for Turkey. Thus, a seismic loading of 0.18 g was applied into the analyze model.

For the stability of slopes, a FOS value that equal or greater than 1.5 is usually preferred for static conditions and a FOS value of 1.1 is required with earthquake effect (KGM 2013). Therefore, a safety factor of 1.1 was considered acceptable for the long-term stability in this study. According to analysis result, the lateral active force generated by the retaining wall has to be higher than 9524 kN to make the region stable (Fig. 11).

Discussion

Cruden and Varnes (1996) reported that the geological, morphological, and physical factors, and factors associated with human activity are the main causes of landslides observed in the world. According to recent studies, landslides in the eastern Black Sea region (EBSR) of Turkey are triggered by dense rainfalls, weathering, high slope angle and anthropogenic impacts. Some of the landslide events occurred in EBSR having similar field characteristics with this study are presented below.

Genc (1993) revealed that the road excavation at the toe of slope and increasing ground water level in the colluvium unit due to the heavy rainfall are the main causing factors of Catak (Trabzon) Landslide. Akgun (2011) reported that the high slope angle, ground water in debris unit and undercutting of the slope toe through river erosion caused an impending failure in Kurtun (Gumushane) District. Avsar et al. (2014) indicated that the Aksu (Giresun) Landslide occurred in completely weathered dasitic tuffs triggered by the road excavation and rising of the ground water level in toe zone. Topsakal and Topal (2015) pointed out that the road excavation and percolations of surface water into the colluvium unit are the main triggering

Fig. 10 Tectonic map of the Turkey showing Black Sea Fault (Modified from Bozkurt 2001)

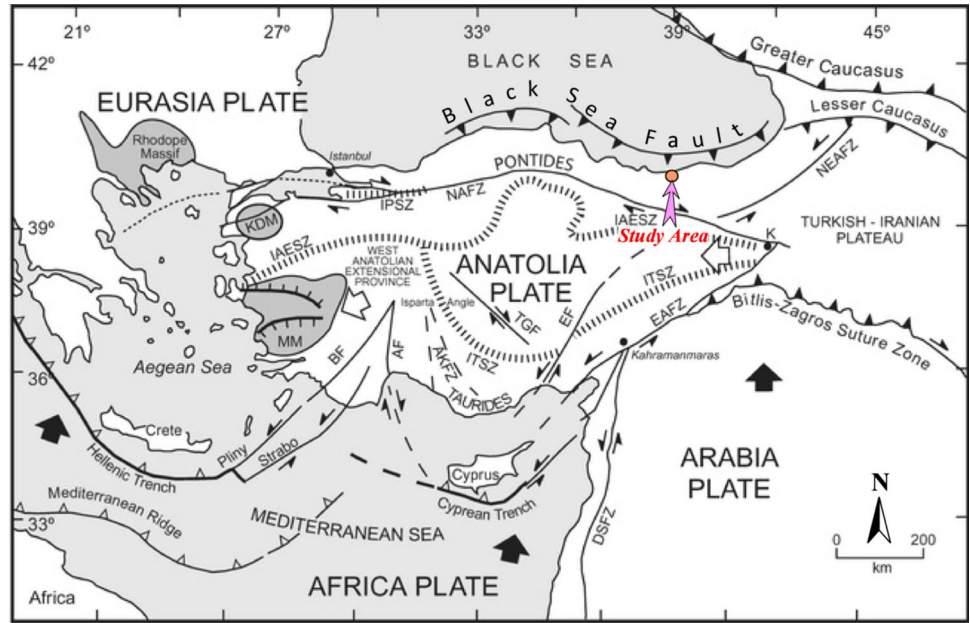
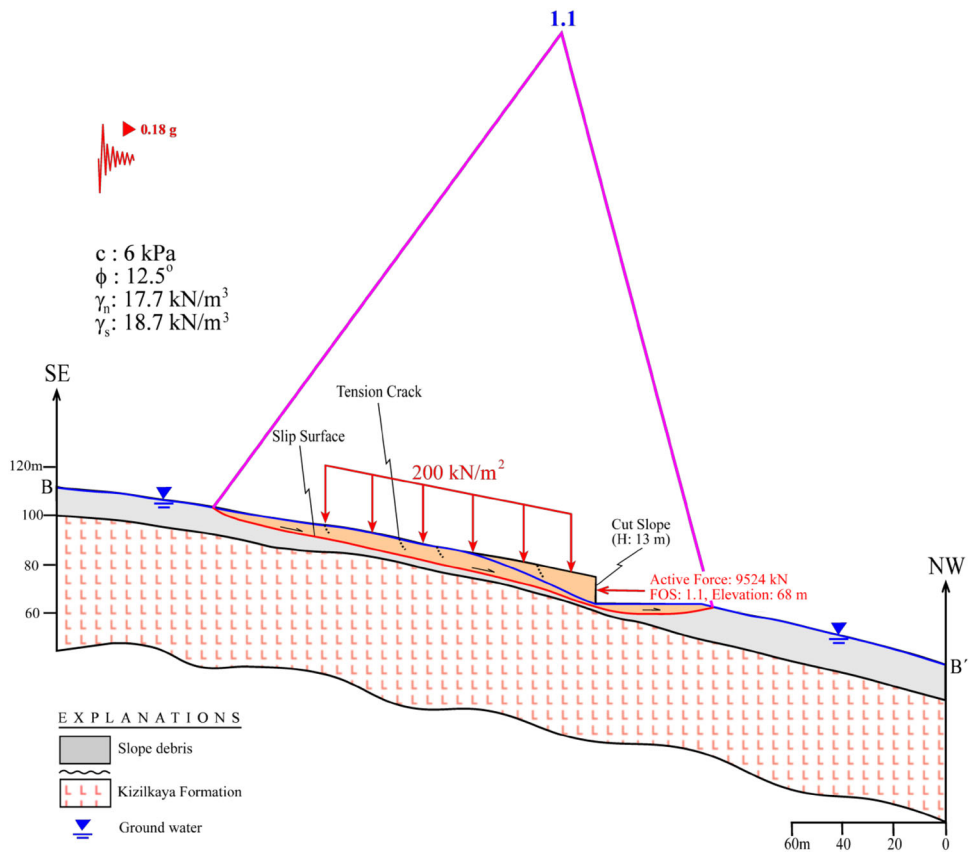


Fig. 11 LE analysis evaluated for determining the lateral active force of retaining wall along the B–B' cross-section



factors of the mass movement occurred in Meydancik (Artvin) Province. Kaya et al. (2016) reported that the mass movement in Gumushane city was encouraged by high-steep slope excavation in debris unit, weathering of the

basement rock (granite), and ground water in the toe of slope.

Inclinometer measurements taken from boreholes indicate that the subsurface location of the mass movement in

the Citlakkale District takes place within the slope debris (Table 2). The ground water level measurements show that the failure surface around the toe zone is beneath the water table (Fig. 5). Following a high steep toe excavation in this zone, the natural stress balance was broken as a result of unloading. Although the failure occurred end of the rainy season, the influence of ground water at the toe zone probably played an additional role on sliding. Throughout the field investigations, it was noticed that the initial tension cracks close to slope face are followed by the next cracks towards the residential area. Considering the LE analysis model for post-excavation case, the slip surfaces with a safety factor smaller than 0.5 concentrate close vicinity of the cut slope (Fig. 8c). The FEM-SSR analysis also shows that a large strain occurs and the plastic zone extends through the slope after an excavation (Fig. 8d). All these indicators prove that the high-steep excavation caused a mass movement starting at the slope and progressing upwards. It is clearly seen that the findings of the present study exactly coincide with the results of the researches mentioned above. Therefore, constantly increasing urbanization and growing population in EBSR cause catastrophic environmental damage such as landslides.

Conclusions

The Citlakkale District is located in Giresun city (NE Turkey), where the slope debris crops out. The geological material of the slope debris is mainly composed of clay, silt, and sand. Immediately after the slope excavation to establish a new settlement in the area, an impending failure occurred in late-March 2014. In order to investigate the causes and the mechanism of this failure, a geotechnical study including engineering geological mapping, field observation, drilling work, geophysical investigation, sampling, laboratory testing, in situ monitoring, and stability analyses of the slope was performed. Inclinometer measurements revealed that the failure mode is composite with very slow velocity and failure started within the slope debris. According to LE and FEM-SSR analyses, it was determined that the slope having natural topographical geometry was stable, but it loses stability following the steep slope excavation over the critical height of 6.5 m. Therefore, a measurement is necessary for the long-term stability of slope. Application of a retaining wall with a lateral active force higher than 9524 kN may prevent the landslide movement and stabilize the area. In this study, the anthropogenic effect in the site was determined to be the most efficient factor caused the failure. This study also reveals that use of the different methods in slope stability studies has an extremely important role in understanding

the generation mechanism of mass movements, and determination of the reliable and realistic precautions.

Acknowledgments Author would like to express their sincerest gratitude to the editor, reviewers, Dr. Zülfi Gürocak and Dr. Selçuk Alemdağ for their excellent comments. Thanks are due to the Academic Writing and Translation Office of RTE University and Dr. Kadir Karaman for improving the language of the manuscript. The author gratefully acknowledges Geological Engineer Köksal Akın for the field work associated with this study.

References

- Abramson LW, Lee TS, Sharma S, Boyce GM (2001) Slope stability and stabilization methods, 2nd edn. Wiley, New York, p 736
- AFAD (2016) Republic of Turkey Prime Ministry Disaster and Emergency Management Authority. <http://www.deprem.gov.tr/en/eventcatalogue>. Accessed 30 Apr 2016
- Akgun A (2011) Assessment of possible damaged areas due to landslide-induced waves at a constructed reservoir using empirical approaches: Kurtun (North Turkey) dam reservoir area. *Nat Hazards Earth Syst Sci* 11(5):1341–1350
- Akgun A, Bulut F (2007) GIS-based landslide susceptibility for Arsin-Yomra (Trabzon, North Turkey) region. *Environ Geol* 51:1377–1387
- Akgun A, Dag S, Bulut F (2008) Landslide susceptibility mapping for a landslide-prone area (Findikli, NE of Turkey) by likelihood-frequency ratio and weighted linear combination models. *Environ Geol* 54:1127–1143
- Alemdag S, Kaya A, Karadag M, Gurocak Z, Bulut F (2013) Utilization of limit equilibrium method for the stability analysis of debris: an example of the Kalebasi District (Gumushane). *Cumhur Earth Sci J* 30(2):49–62
- Alemdag S, Akgun A, Kaya A, Gokceoglu C (2014) A large and rapid planar failure: causes, mechanism and consequences (Mordut, Gumushane, Turkey). *Arab J Geosci* 7:1205–1221
- Alemdag S, Kaya A, Karadag M, Gurocak Z, Bulut F (2015) Utilization of the limit equilibrium and finite element methods for the stability analysis of the slope debris: an example of the Kalebasi district (NE Turkey). *J Afr Earth Sc* 106:134–146
- ASTM (2009a) Standard test methods for particle-size distribution (gradation) of soils using sieve analysis. ASTM D6913-04(2009)e1, West Conshohocken, PA
- ASTM (2009b) Standard test methods for laboratory determination of density (unit weight) of soil specimens. ASTM D7263-09, West Conshohocken, PA
- ASTM (2010) Standard test methods for liquid limit, plastic limit, and plasticity index of soils. ASTM D4318-10e1, West Conshohocken, PA
- ASTM (2011a) Standard practice for classification of soils for engineering purposes (Unified Soil Classification System). ASTM D2487-11, West Conshohocken, PA
- ASTM (2011b) Standard test method for consolidated undrained triaxial compression test for cohesive soils. ASTM D4767-11, West Conshohocken, PA
- Avsar O, Akgun H, Kockar MK (2014) Investigation of the failure mechanism and stabilization of a landslide in weathered tuffite, Giresun, northeastern Turkey. *Environ Earth Science* 72:3723–3740
- Bishop AW (1955) The use of the slip circle in the stability analysis of slopes. *Geotechnique* 5:7–17
- Bishop AW, Morgenstern N (1960) Stability coefficients for earth slopes. *Geotechnique* 10(4):129–150

- Bowles JE (1988) Foundation analysis and design. McGraw-Hill Book Company, New York
- Bozkurt E (2001) Neotectonics of Turkey—a synthesis. *Geodin Acta* 14(1):3–30
- Bulut F, Boynukalın S, Tarhan F, Ataoglu E (2000) Reliability of landslide isopleth maps. *Bull Eng Geol Environ* 58:95–98
- Cruden DM, Varnes DJ (1996) Landslide types and processes. *Landslides: investigation and mitigation*. Transportation Research Board, special report, p 247
- Duncan JM, Wright SG (2005) Soil strength and slope stability. Wiley, New York, p 297
- Fahimifar A, Abdolmaleki A, Soltani P (2013) Stabilization of rock slopes using geogrid boxes. *Arab J Geosci* 7(2):609–621
- Fell R, Walker BF, Finlay PJ (1996) Estimating the probability of landsliding. In: Proc. 7th Australian New Zealand conference on geomechanics, Adelaide, Institution of Engineers Australia, Canberra, pp 304–311
- Fellenius W (1936) Calculation of the stability of earth dams. In: Proc. transactions of the 2nd Congress on Large Dams, International Commission on Large Dams of the World Power Conference 4, pp 445–462
- Genc S (1993) Structural and geomorphological aspects of the Catak landslide, NE Turkey. *Q J Eng Geol Hydrogeol* 26(2):99–108
- Griffiths DV, Lane PA (1999) Slope stability analysis by finite elements. *Geotechnique* 49(3):387–403
- Guven IH (1993) 1/25000 Scale geology map of eastern Pontides. Mineral Research and Exploration Institute of Turkey (MTA) Publication
- Guzzetti F, Carrara A, Cardinali M, Reichenbach P (1999) Landslide hazard evaluation: a review of current techniques and their application in a multi-scale study, Central Italy. *Geomorphology* 31:181–216
- Hammah RE, Yacoub TE, Curran JH (2006) Investigating the performance of the shear strength reduction (SSR) method on the analysis of reinforced slopes. In: Proceedings of the 59th Canadian Geotechnical Conference, Vancouver
- Hart RD, Detournay C, Cundall PA (2008) Continuum and distinct element modeling in geo-engineering. In: Cundall PA (ed) Proceedings First FLAC/DEM symposium, Minneapolis, p 698
- Janbu N (1954a) Application of composite slip surface for stability analysis. In: Proc. European conference on stability of earth slopes 3, pp 43–49
- Janbu N (1954b) Stability analysis of slopes with dimensionless parameters. Soil mechanics series, no. 46. Harvard University, Cambridge
- Janbu N (1968) Slope stability computations, soil mechanics and foundation engineering report. The Technical University of Norway, Trondheim
- Janbu N (1973) Slope stability computations, embankment-dam engineering, vol Casagrande. Wiley, New York
- Karaman K (2013) Evaluation of rock slope stability by different methods (Unye, Ordu). *J Geol Eng* 37:27–47
- Karaman K, Ercikdi B, Kesimal A (2013) The assessment of slope stability and rock excavatability in a limestone quarry. *Earth Sci Res J* 17:169–181
- Karsli F, Atasoy M, Yalcin A, Reis S, Demir O, Gokceoglu C (2009) Effects of land-use changes on landslides in a landslide-prone area (Ardesen, Rize, NE Turkey). *Environ Monit Assess* 156:241–255
- Kaya A, Akgün A, Karaman K, Bulut F (2015) Understanding the mechanism of a slope failure on nearby a highway tunnel route by different slope stability analysis methods: a case from NE Turkey. *Bull Eng Geol Environ*. doi:10.1007/s10064-015-0770-5
- Kaya A, Alemdag S, Dag S, Gurocak Z (2016) Stability assessment of high-steep cut slope debris on a landslide (Gumushane, NE Turkey). *Bull Eng Geol Environ* 1(75):89–99
- Kesimal A, Ercikdi B, Cihangir F (2008) Environmental impacts of blast-induced acceleration on slope instability at a limestone quarry. *Environ Geol* 54:381–389
- Ketin I (1966) Tectonic units of Anatolia. *J Gen Dir Miner Res Explor (MTA)* 66:23–34
- KGM (2013) Specification for highway works (in Turkish). Turk Gen Dir Highw, Ankara
- Li X (2007) Finite element analysis of slope stability using a nonlinear failure criterion. *Comput Geotech* 34:127–136
- Lowe J, Karafiath L (1959) Stability of earth dams upon drawdown. In: Proc. 1st PanAmerican conference on soil mechanics and foundation engineering 2, pp 537–552
- Mohr O (1900) Welche umstände bedingen die elastizitätsgrenze und den bruch eines materials? *Zeit Deut Ing* 44:1524–1530
- Morgenstern NR, Price VE (1967) A numerical method for solving the equations of stability of general slip surfaces. *Comput J* 9(4):388–393
- Nefeslioglu H, Gokceoglu C (2011) Probabilistic risk assessment in medium scale for rainfall-induced earthflows: Catakli catchment area (Cayeli, Rize, Turkey). *Math Probl Eng* 2011:1–21
- Nefeslioglu H, Gokceoglu C, Sonmez H, Gorum T (2011) Medium-scale hazard mapping for shallow landslide initiation: the Buyukoy catchment area (Cayeli, Rize, Turkey). *Landslides* 8:459–483
- Ontigao JAR, Sayao ASFJ (2004) Handbook of slope stabilization. Springer, Berlin, p 478
- Osna T, Sezer AE, Akgun A (2014) GeoFIS: an integrated tool for the assessment of landslide susceptibility. *Comput Geosci* 66:20–30
- Reis S, Yalcin A, Atasoy M, Nisanci R, Bayrak T, Erduran M, Sancar C, Ekercin S (2012) Remote sensing and GIS-based landslide susceptibility mapping using frequency ratio and analytical hierarchy methods in Rize province (NE Turkey). *Environ Earth Sci* 66:2063–2073
- Rocscience Inc. (2010) Slide version 6.0 – 2D limit equilibrium slope stability analysis, Toronto, ON. <http://www.roscience.com>
- Rocscience Inc. (2011) Phase² version 8.0 – finite element analysis for excavations and slopes, Toronto, ON. <http://www.roscience.com>
- Sancio RT (1981) The use of back-calculations to obtain shear and tensile strength of weathered rocks. In: Proceedings of the international symposium on weak rock, Tokyo, pp 647–652
- Sarma SK (1973) Stability analysis of embankments and slopes. *Geotechnique* 23(3):423–433
- Shukra R, Baker R (2003) Mesh geometry effects on slope stability calculation by FLAC strength reduction method-linear and non-linear failure criteria. In: Brummer R et al (eds) Proceedings of the 3rd International FLAC Symposium, Sudbury, Ontario, Canada, pp 109–116
- Spencer E (1967) A method of analysis of the stability of embankments assuming parallel inter-slice forces. *Geotechnique* 17(1):11–26
- Topsakal E, Topal T (2015) Slope stability assessment of a re-activated landslide on the Artvin-Savsat junction of a provincial road in Meydancik, Turkey. *Arab J Geosci* 8(3):1769–1786
- Turner KA, Schuster RL (1996) Landslides: investigation and mitigation. National Academy Press, Washington DC, p 672
- Ulusay R, Tuncay E, Sonmez H, Gokceoglu C (2004) An attenuation relationship based on Turkish strong motion data and iso-acceleration map of Turkey. *Eng Geol* 74(3–4):265–291
- USCE (1970) Engineering and design: stability of earth and rock-fill dams. Engineer manual EM 1110-2-1902. Department of the Army, Corps of Engineers, Office of the Chief of Engineers, Washington DC

- Varnes DJ (1978) Slope movement types and processes. TRB Natl Res Counc Spec Rep 176:11–33
- Yalcin A (2008) GIS-based landslide susceptibility mapping using analytical hierarchy process and bivariate statistics in Ardesen (Turkey): comparisons of results and confirmations. *Catena* 72:1–12
- Yalcin A, Bulut F (2007) Landslide susceptibility mapping using GIS and digital photogrammetric techniques: a case study from Ardesen (NE-Turkey). *Nat Hazards* 41:201–226